PLOS GENETICS

RESEARCH ARTICLE

Satellite DNA-containing gigantic introns in a unique gene expression program during *Drosophila* spermatogenesis

Jaclyn M. Fingerhut[1,2], **Jessica V. Moran**[2], **Yukiko M. Yamashita**[1,2,3,4]*

1 Cellular and Molecular Biology Program, University of Michigan, Ann Arbor, Michigan, United States of America, **2** Life Sciences Institute, University of Michigan, Ann Arbor, Michigan, United States of America, **3** Department of Cell and Developmental Biology, University of Michigan, Ann Arbor, Michigan, United States of America, **4** Howard Hughes Medical Institute, University of Michigan, Ann Arbor, Michigan, United States of America

* yukikomy@umich.edu

OPEN ACCESS

Citation: Fingerhut JM, Moran JV, Yamashita YM (2019) Satellite DNA-containing gigantic introns in a unique gene expression program during *Drosophila* spermatogenesis. PLoS Genet 15(5): e1008028. https://doi.org/10.1371/journal.pgen.1008028

Editor: Giovanni Bosco, Geisel School of Medicine at Dartmouth, UNITED STATES

Received: December 20, 2018

Accepted: February 18, 2019

Published: May 9, 2019

Data Availability Statement: All relevant data are within the manuscript and its Supporting Information files.

Funding: This work was supported by the Howard Hughes Medical Institute (to YMY, https://www.hhmi.org) and the NIH Cellular and Molecular Biology Training Grant T32-GM007315 (to JMF, https://www.nih.gov). The funders had no role in study design, data collection and analysis, decision to publish, or preparation of the manuscript.

Abstract

Intron gigantism, where genes contain megabase-sized introns, is observed across species, yet little is known about its purpose or regulation. Here we identify a unique gene expression program utilized for the proper expression of genes with intron gigantism. We find that two *Drosophila* genes with intron gigantism, *kl-3* and *kl-5*, are transcribed in a spatiotemporal manner over the course of spermatocyte differentiation, which spans ~90 hours. The introns of these genes contain megabases of simple satellite DNA repeats that comprise over 99% of the gene loci, and these satellite-DNA containing introns are transcribed. We identify two RNA-binding proteins that specifically localize to *kl-3* and *kl-5* transcripts and are needed for the successful transcription or processing of these genes. We propose that genes with intron gigantism require a unique gene expression program, which may serve as a platform to regulate gene expression during cellular differentiation.

Author summary

Introns are non-coding elements of eukaryotic genes, often containing important regulatory sequences. Curiously, some genes contain introns so large that more than 99% of the gene locus is non-coding. One of the best-studied large genes, Dystrophin, a causative gene for Duchenne Muscular Dystrophy, spans 2.2Mb, only 11kb of which is coding. This phenomenon, 'intron gigantism', is observed across species, yet little is known about its purpose or regulation. Here we identify a unique gene expression program utilized for the proper expression of genes with intron gigantism using *Drosophila* spermatogenic genes a model system. We show that the gigantic introns of these genes are transcribed in line with the exons, likely as a single transcript. We identify two RNA-binding proteins that specifically localize to the site of transcription and are needed for the successful transcription or processing of these genes. We propose that genes with intron gigantism require a unique gene expression program, which may serve as a platform to regulate gene expression during cellular differentiation.

Competing interests: The authors have declared that no competing interests exist.

Introduction

Introns, non-coding elements of eukaryotic genes, often contain important regulatory sequences and allow for the production of diverse proteins from a single gene, adding critical regulatory layers to gene expression [1]. Curiously, some genes contain introns so large that more than 99% of the gene locus is non-coding. In humans, neuronal and muscle genes are enriched amongst those with the largest introns [2]. One of the best-studied large genes, Dystrophin, a causative gene for Duchenne Muscular Dystrophy, spans 2.2Mb, only 11kb of which is coding. A large portion of the remaining non-coding sequence is comprised of introns rich in repetitive DNA [3]. While intron size ('gigantism') is conserved between mouse and human, there is little sequence conservation within the introns, implying the functionality of intron gigantism [4].

The *Drosophila* Y chromosome provides an excellent model for studying intron gigantism. Approximately 80% of the 40Mb Y chromosome is comprised of repetitive sequences, primarily satellite DNAs, which are short tandem repeats, such as $(AATAT)_n$ (Fig 1A)[5–8]. The *Drosophila* Y chromosome encodes fewer than 20 genes [9], six of which are classically known as the 'fertility factors' [10–13]. One of these fertility factors, *kl-3*, which encodes an axonemal dynein heavy chain [14–16], spans at least 4.3Mb [11, 17, 18], while its coding sequence is only ~14kb (Fig 1A). This is due to the large satellite DNA rich-introns, some of which are megabases in size, that comprise more than 99% of the *kl-3* locus. The other five fertility factors (*kl-1*, *kl-2*, *kl-5*, *ks-1*, *ks-2*), have a similar gene structure, possessing large introns of repetitive satellite DNAs [11]. These six large Y chromosome genes are solely expressed during spermatogenesis [14, 19, 20].

In the *Drosophila* testis, germ cells undergoing differentiation are arranged in a spatiotemporal manner, where the germline stem cells (GSCs) reside at the very apical tip and differentiating cells are gradually displaced distally (Fig 1B) [21]. GSC division gives rise to spermatogonia (SG), which undergo four mitotic divisions with incomplete cytokinesis to become a cyst of 16 SGs. 16-cell SG cysts enter meiotic S phase, at which point they become known as spermatocytes (SCs). SCs have an extended G2 phase, spanning 80–90 hours, prior to initiation of the meiotic divisions [22]. During this G2 phase, the cells increase approximately 25 times in volume and the homologous chromosomes pair and partition into individual chromosome territories (Fig 1C) [23, 24]. During this period, SCs transcribe the majority of genes whose protein products will be needed for meiotic division and spermiogenesis [25–27]. Gene expression in SCs is thus tightly regulated to allow for timely expression of meiotic and spermiogenesis genes [28].

It has long been known that three of the Y-chromosome-associated genes that contain gigantic introns (*kl-5*, *kl-3* and *ks-1*, Fig 1A) form lampbrush-like nucleoplasmic structures in SCs, named Y-loops [denoted as loops A (*kl-5*), B (*kl-3*), and C (*ks-1*), (Fig 1C and 1D)] [17]. Y-loop structures reflect the robust transcription of underlying genes, and have been observed across Drosophilids, including *D. simulans*, *D. yakuba*, *D. pseudoobscura*, *D. hydei* and *D. littoralis* [29, 30]. Much of the fundamental knowledge about Y-loops comes from *D. hydei*, which forms large, cytologically distinct Y-loops [31], leading to the discovery that these structures are formed by the transcription of large loci comprised of repetitive DNAs [32–37]. Interestingly, in *D. pseudoobscura*, which contains a 'neo-Y' (not homologous to the ancestral Y chromosome), Y-loops are thought to be formed by Y-linked genes instead of by the *kl-3*, *kl-5* and *ks-1* homologs, which are autosomal [38], suggesting that Y-loop formation is a unique characteristic of Y-linked genes, instead of being a gene-specific phenomenon.

The transcription/processing of such gigantic genes/RNA transcripts, in which exons are separated by megabase-sized introns, must pose a significant challenge for cells. However, how

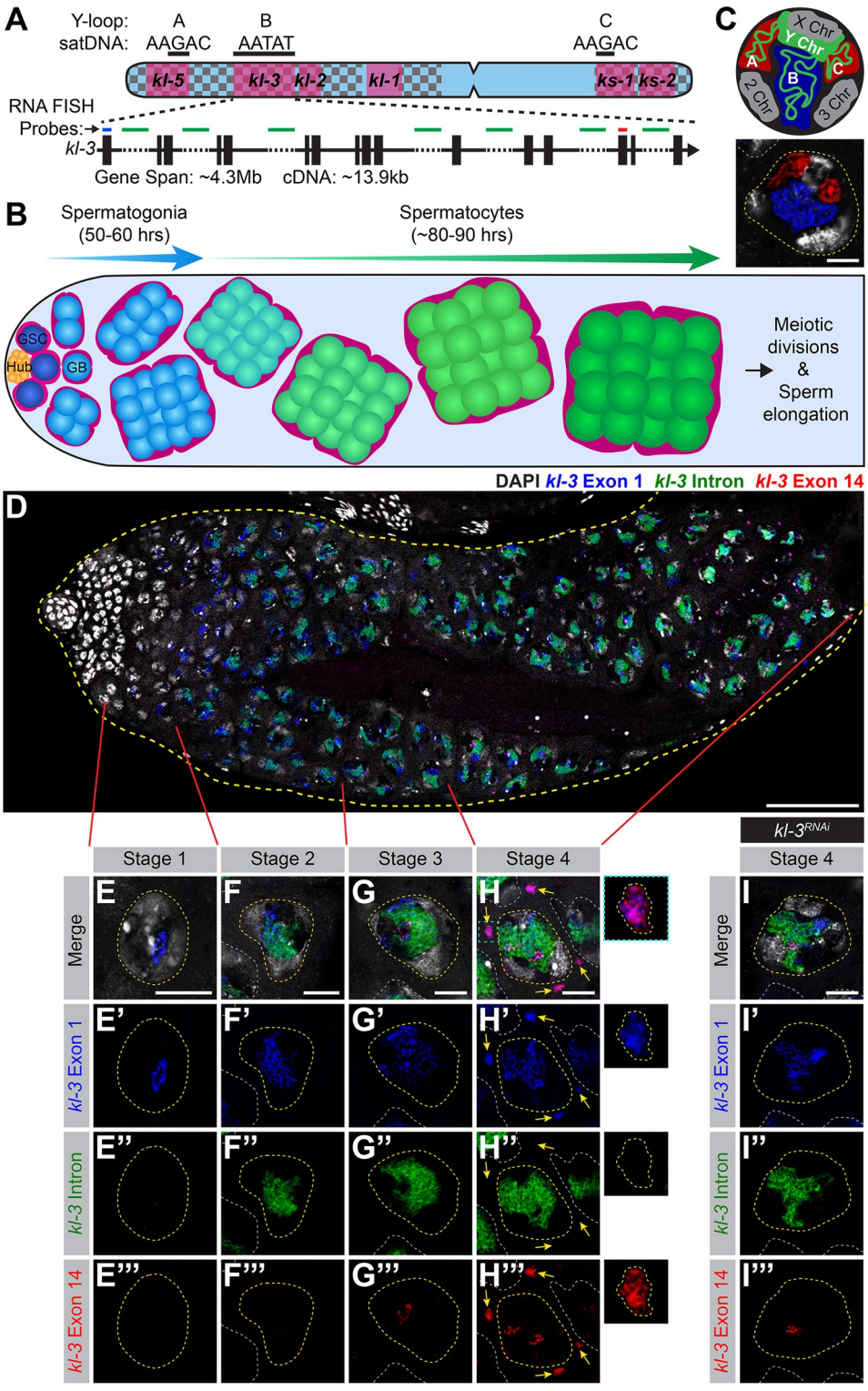

Fig 1. The Y-loop gene *kl-3* is expressed in a spatiotemporal manner during SC development. (A) Diagram of the *Drosophila* Y chromosome. Regions enriched for satellite DNA (checkered pattern), locations of the fertility factor genes (magenta) and the Y-loop forming regions (black bars) with associated satellite DNA sequences are indicated. Enlarged is a diagram of the Y-loop B gene *kl-3*. Exons (vertical rectangles), introns (black line), intronic satellite DNA repeats (dashed line) and regions of *kl-3* targeted by RNA FISH probes (colored bars). (B) Diagram of *Drosophila* spermatogenesis: GSCs (attached to the hub) produce mitotically-amplifying SGs, which become SCs. SCs develop

over an 80–90 hour G2 phase before initiating the meiotic divisions. (C) Top: SC nucleus model showing the Y-loops in the nucleoplasm. DNA (white), Y chromosome (green), Y-loops A and C (red) and Y-loop B (blue). Bottom: RNA FISH for the Y-loop gene intronic transcripts in a SC nucleus. Y-loops are visualized using probes for Y-loops A and C (Cy3-$(AAGAC)_6$, red) and Y-loop B (Cy5-$(AATAT)_6$, blue). DAPI (white), SC nucleus (yellow dashed line) and nuclei of neighboring cells (white dashed line). Bar: 10μm. (D-H) RNA FISH to visualize *kl-3* expression in wildtype testes. Exon 1 (blue), *kl-3* intron (Alexa488-$(AATAT)_6$, green), Exon 14 (red) and DAPI (white). (D) Apical third of the testis through the end of SC development (yellow dashed line). Bar: 75μm. (E-H) Single SC nuclei (yellow dashed line) at each stage of *kl-3* expression. Nuclei of neighboring cells (white dashed line) and cytoplasmic mRNA granules (yellow arrows). Bar: 10μm. Inset: *kl-3* mRNA granule (yellow dashed line). (I) RNA FISH against *kl-3* following *kl-3* RNAi (*bam-gal4>UAS-kl-3*$^{TRiP.HMC03546}$). Single late SC nucleus (yellow dashed line) and nuclei of neighboring cells (white dashed line). Bar: 10μm.

https://doi.org/10.1371/journal.pgen.1008028.g001

genes with intron gigantism are expressed and whether intron gigantism plays any regulatory roles in gene expression remain largely unknown. In this study, we began addressing these questions by using the Y-loop genes as a model, and describe the unusual nature of the gene expression program associated with intron gigantism. We find that transcription of Y-loop genes progresses in a strictly spatiotemporal manner, encompassing the entire ~90 hours of SC development: the initiation of transcription occurs in early SCs, followed by the robust transcription of the satellite DNA from the introns, with cytoplasmic mRNA becoming detectable only in late SCs. We identify two RNA-binding proteins, Blanks and Hephaestus (Heph), which specifically localize to the Y-loops, and show that they are required for robust transcription and/or proper processing of the Y-loop gene transcripts. Mutation of the *blanks* or *heph* genes leads to sterility due to the loss of Y-loop gene products. Our study demonstrates that genes with intron gigantism require specialized RNA-binding proteins for proper expression. We propose that such unique processing may be utilized as an additional regulatory mechanism to control gene expression during differentiation.

Results

Transcription of a Y-loop gene, *kl-3*, is spatiotemporally organized

To start to investigate how the expression of Y-loop genes may be regulated, we sought to monitor their expression during SC development. In previous studies using *D. hydei*, when two differentially-labeled probes against two intronic repeats of the Y-loop gene *DhDhc7(y)* (homologous to *D. melanogaster kl-5*) were used for RNA fluorescent *in situ* hybridization (FISH), expression of the earlier repeat preceded that of the later repeat [39, 40], leading to the idea that Y-loop genes might be transcribed as single, multi-megabase, transcripts. Consistently, Miller spreading of SC Y chromosomes, in which transcripts can be seen still bound to DNA, showed the long Y-loop transcripts [41, 42]. However, transcription of the exons was not visualized and extensive secondary structures were present in the Miller spreads, leaving it unclear whether the entire gene region is transcribed as a single transcript.

By using differentially-labeled probe sets designed for RNA FISH to visualize 1) the first exon, 2) the satellite DNA $(AATAT)_n$ repeats found in multiple introns including the first [5, 43], and 3) exon 14 (of 16) of *kl-3* (Fig 1A, S1 File), we found that *kl-3* transcription is organized in a spatiotemporal manner: transcript from the first exon becomes detectable in early SCs, followed by the expression of the $(AATAT)_n$ satellite from the introns, then finally by the transcript from exon 14 in more mature SCs (Fig 1D). These results suggest that transcription of *kl-3* takes the entirety of SC development, spanning ~90 hours. The pattern of transcription is consistent with the model proposed for Y-loop gene expression in *D. hydei*: the gene is likely transcribed as a single transcript that contains the exons and gigantic introns, although we cannot exclude the possibility of other mechanisms, such as the trans-splicing of multiple individually transcribed exons [44].

Based on the expression pattern of early exon, $(AATAT)_n$ satellite-containing introns, and late exon, SC development can be subdivided into four distinct stages (Fig 1E–1H). In stage 1, only exon 1 transcript is apparent (Fig 1E). In stage 2, the expression of intron transcript is detectable, and the signal from exon 1 remains strong (Fig 1F). Stage 3 is defined by the addition of late exon signal in addition to the continued presence of exon 1 and intron transcripts, indicating that transcription is nearly complete (Fig 1G). Stage 4 is characterized by the presence of exon probe signals in granule-like structures in the cytoplasm (Fig 1H), which likely reflect *kl-3* mRNA localizing to ribonucleoprotein (RNP) granules, as they never contain intron probe signal. These granules are absent following RNAi-mediated knockdown of *kl-3* (*bam-gal4>UAS-kl-3*$^{TRiP.HMC03546}$, Fig 1I), confirming that they reflect *kl-3* mRNA. The same pattern of expression was seen for the Y-loop gene *kl-5* (see below), suggesting that transcription of the other Y-loop genes proceeds in a similar manner.

Together, these results show that the gigantic Y-loop genes, including megabases of intronic satellite DNA repeats, are transcribed continuously in a process that spans the entirety of SC development, culminating in the formation of mRNA granules in the cytoplasm near the end of the 80–90 hour meiotic G2 phase. While transcription elongation is believed to be quite stable [45], the presence of tandem arrays [46] or repeat expansions (as seen in trinucleotide expansion diseases) [47–49] can greatly slow an elongating polymerase and/or lead to premature dissociation [50]. Therefore, Y-loop gene transcription may require precise regulation.

Identification of genes that may regulate the transcription of the Y-loop genes

Considering the size of the Y-loop gene loci and their satellite DNA-rich introns, transcription of the Y-loop genes likely utilizes unique regulatory mechanisms. To start to understand such a genetic program, we performed a screen (See Methods and S2 File). Briefly, a list of candidates was curated using a combination of gene ontology (GO) terms, expression analysis, predicted functionality and reagent availability, resulting in a final list of 67 candidate genes (S2 File). Candidates were screened for several criteria including protein localization, fertility, and Y-loop gene expression. Among these, two genes, *blanks* and *hephaestus (heph)*, exhibit localization patterns and phenotypes that reveal critical aspects of Y-loop gene regulation and were further studied. Several proteins, including Boule [51], Hrb98DE [52], Pasilla [52, 53] and Rb97D [54], were previously shown to localize to the Y-loops but displayed no detectable phenotypes in Y-loop gene expression in SCs using RNAi-mediated knockdown and/or available mutants (S2 File), and were not further pursued in this study.

Blanks and Heph are RNA binding proteins that specifically localize to the Y-loops and are required for fertility

Blanks, a RNA-binding protein with multiple dsRNA binding domains, is primarily expressed in SCs. Blanks has been shown to be important for post-meiotic sperm development and male fertility [55, 56], and Blanks' ability to bind RNA was found to be necessary for fertility [55]. In order to assess Blanks' localization within the SC nucleus, testes expressing GFP-Blanks were processed for RNA FISH with probes against the intronic satellite DNA transcripts [$(AATAT)_n$ for Y-loop B/*kl-3*, $(AAGAC)_n$ for Y-loops A/*kl-5* and C/*ks-1* [57]]. $(AATAT)_n$ is the only satellite DNA found in Y-loop B [5, 58] and while $(AAGAC)_n$ is not the only satellite DNA found in Y-loops A & C, its expression from these loci was previously characterized [57]. We found that GFP-Blanks exhibits strong localization to Y-loop B (Fig 2A).

Heph, a heterogeneous nuclear ribonucleoprotein (hnRNP) homologous to mammalian polypyrimidine track binding protein (PTB), is a RNA-binding protein with multiple RNA

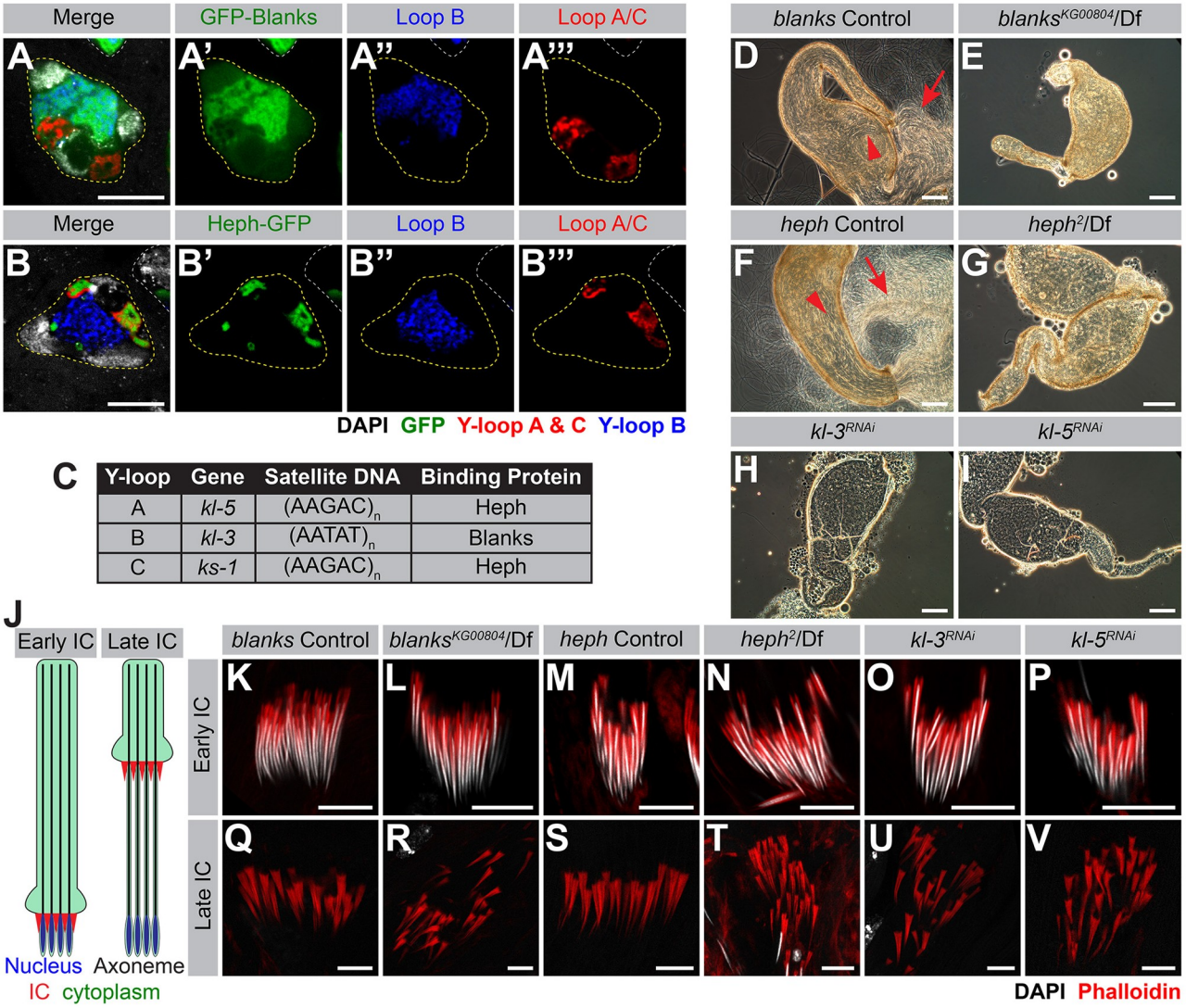

Fig 2. Blanks and Heph localize to the Y-loops and are required for fertility. (A, B) RNA FISH against the Y-loop gene intronic transcripts in flies expressing GFP-Blanks (A) or Heph-GFP (B). Y-loops A and C (Cy3-$(AAGAC)_6$, red), Y-loop B (Cy5-$(AATAT)_6$, blue), GFP (green), SC nucleus (yellow dashed line) and nuclei of neighboring cells (white dashed line). Bar: 10μm. (C) Table listing Y-loop designation, associated gene, the satellite DNA repeats found within the introns and whether the Y-loop is bound by Heph or Blanks. (D-I) Phase contrast images of seminal vesicles in *blanks* controls (C), $blanks^{KG00084}$/Df (D), *heph* controls (E), $heph^{2}$/Df (F), *bam-gal4>UAS-kl-3*$^{TRiP.HMC03546}$ (G) and *bam-gal4>UAS-kl-5*$^{TRiP.HMC03747}$ (H). Sperm within the seminal vesicle (red arrowhead) and extruded sperm (red arrow). Bar: 100μm. (J) Schematic of IC progression during individualization—in this diagram, the direction of IC progression is from bottom to top. Nucleus (blue), axoneme (black), ICs (red) and cytoplasm (green). (K-V) Phalloidin staining of early ICs (K-P) and late ICs (Q-V) in indicated genotypes. Phalloidin (actin, red) and DAPI (white). Bar: 10μm.

https://doi.org/10.1371/journal.pgen.1008028.g002

recognition motifs (RRMs) that is expressed in the testis [59]. Heph has also been implicated in post-meiotic sperm development and male fertility [60, 61]. By using a Heph-GFP protein trap (p(PTT-GC)$heph^{CC00664}$) combined with RNA FISH to visualize the Y-loop gene intronic transcripts, we found that Heph-GFP localizes to Y-loops A and C (Fig 2B). It should be noted that the *heph* locus encodes 25 isoforms and the Heph-GFP protein trap likely represents only a subset of *heph* gene products. A summary of Y-loop designation, gene, intronic satellite DNA repeat, and binding protein is provided in Fig 2C.

We confirmed previous reports that *blanks* is required for male fertility [55, 56]. By examining the seminal vesicles for the presence of motile sperm, we found that seminal vesicles from

control siblings contain abundant motile sperm (Fig 2D, 13% empty, 87% normal, n = 46) while seminal vesicles from *blanks* mutants (*blanks*^{KG00084}/Df(3L)BSC371) lack motile sperm (Fig 2E, 96% = empty, 4% greatly reduced, n = 58). We also confirmed previous reports that *heph* is required for fertility [60, 62]. Seminal vesicles from *heph* mutants (*heph*^{2}/Df(3R) BSC687) also lack motile sperm (Fig 2G, 100% empty, n = 21), while those from control siblings contain motile sperm (Fig 2F, 5% empty, 95% normal, n = 57).

Previous studies [55, 56, 60] reported that *blanks* and *heph* mutants are defective in sperm individualization, one of the final steps in sperm maturation, where 64 interconnected spermatids are separated by individualization complexes (ICs) that form around the sperm nuclei and migrate in unison along the sperm tails, removing excess cytoplasm and encompassing each cell with its own plasma membrane (Fig 2J) [63]. When the F-actin cones of IC were visualized by Phalloidin staining, it became clear that ICs form properly in all genotypes (Fig 2K–2N), but become disorganized in the late ICs in *blanks* and *heph* mutants, a hallmark of axoneme formation defects [64], preventing completion of individualization (Fig 2Q–2T).

The sterility and individualization defects observed in *blanks* and *heph* mutants are reminiscent of the phenotypes observed in flies lacking axonemal dynein genes including *kl-5* and *kl-3*, the Y-loop A and B genes [14–16, 64–66]. Upon RNAi mediated knockdown of *kl-3* and *kl-5* (*bam-gal4>UAS-kl-3*$^{TRiP.HMC03546}$ or *bam-gal4>UAS-kl-5*$^{TRiP.HMC03747}$), motile sperm are not found in the seminal vesicles (Fig 2H and 2I, *kl-3*: 100% empty, n = 81, *kl-5*: 94% empty, 6% greatly reduced, n = 50) and a scattering of late ICs is observed (Fig 2O, 2P, 2U and 2V). Based on these observations, we hypothesized that the sterility and IC defects observed in *blanks* and *heph* mutants may arise due to failure in the expression of the Y-loop genes.

blanks is required for transcription of the Y-loop B gene *kl-3*

As *blanks* was found to localize to Y-loop B, we first determined whether there were any overt defects in Y-loop B formation or *kl-3* expression in *blanks* mutants. To this end, we performed RNA FISH to visualize the Y-loop gene intronic transcripts in *blanks* mutants. Compared to control testes where intronic satellite DNA transcripts from all Y-loops become detectable fairly early in SC development and quickly reach full intensity (Fig 3A), the signal from the Y-loop B intronic transcripts remains faint in *blanks* mutants (Fig 3B). The expression of Y-loops A and C is comparable between control and *blanks* mutant testes (Fig 3A and 3B).

In addition to a reduction in the expression of the intronic satellite DNA repeats of Y-loop B/*kl-3*, expression of *kl-3* exons is also reduced in *blanks* mutants. By performing RNA FISH using exonic and intronic $(AATAT)_n$ probes for Y-loop B/*kl-3*, we found that *blanks* mutants display an overall reduction in signal intensity for both intronic satellite repeats and exons compared to controls (Fig 3C and 3E). Moreover, cytoplasmic *kl-3* mRNA granules are rarely detected in *blanks* mutants (Fig 3F). The same results are obtained following RNAi mediated knockdown of *blanks* (*bam-gal4>UAS-blanks*$^{TRiP.HMS00078}$, S1 Fig). These results suggest that *blanks* is required for robust and proper expression of Y-loop B/*kl-3* and for the production of *kl-3* mRNA granules, likely at the transcriptional level. Consistently, we found that the amount of Kl-3 protein is greatly diminished in *blanks* mutants, confirming that *blanks* is required for proper expression of Y-loop B/*kl-3* (Fig 3G).

To obtain a more quantitative measure of *kl-3* expression levels in control and *blanks* mutant testes, we performed RT-qPCR. Primers were designed to amplify early (close to the 5' end), middle, and late (close to the 3' end) regions of *kl-3*. For each region, two sets of primers were designed: one primer set spanned a satellite DNA-containing large intron and another spanned a normal size intron (Fig 3H, bars denote spanned intron, and S3 File). All primer sets show a detectable drop in *kl-3* mRNA levels in *blanks* mutants when normalized to

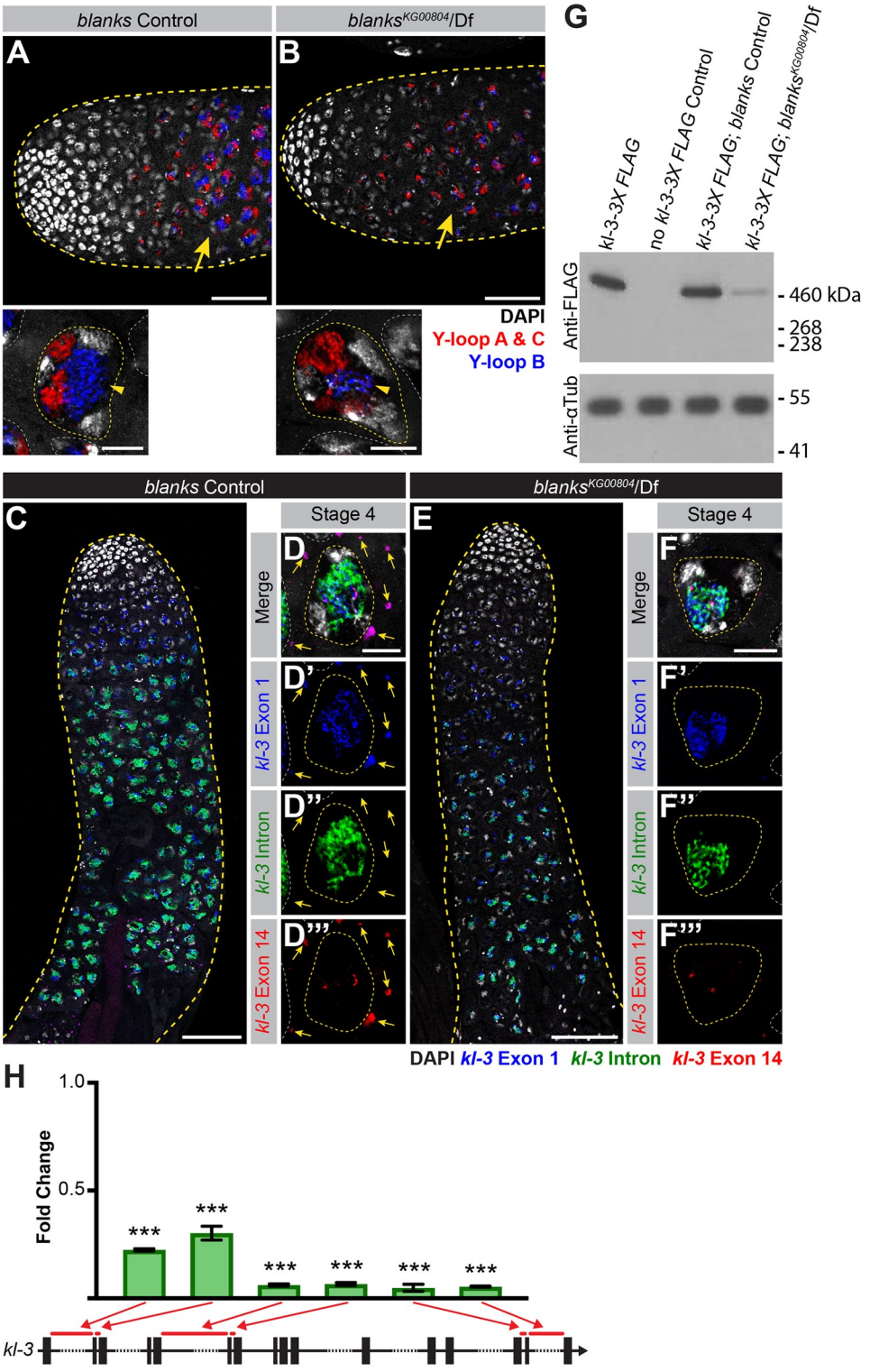

Fig 3. *blanks* is required for *kl-3* expression. (A, B) RNA FISH against the Y-loop gene intronic transcripts in *blanks* control (A) and *blanks*^{KG000804}/Df (B). Testis outline (yellow dashed line), Y-loops A and C (Cy3-$(AAGAC)_6$, red), Y-loop B (Cy5-$(AATAT)_6$, blue) and DAPI (white). Comparable stage SCs are indicated by yellow arrows. Bar: 50μm. High magnification images of single SCs at a comparable stage are provided below. SC nuclei (yellow dashed line) and nuclei of neighboring cells (white dashed line). Bar: 10μm. (C-F) RNA FISH against *kl-3* in *blanks* control (C, D) and *blanks*^{KG00084}/Df (E, F). Exon 1 (blue), *kl-3* intron (Alexa488-$(AATAT)_6$, green), Exon 14 (red) and DAPI (white). (C,

E) Apical third of the testis through the end of SC development (yellow dashed line). Bar: 75μm. (D, F) Single late SC nucleus (yellow dashed line). Nuclei of neighboring cells (white dashed line) and mRNA granules (yellow arrows). Bar: 10μm. (G) Western blot for Kl-3-3X FLAG in the indicated genotypes. The FLAG tag was inserted at the endogenous *kl-3* locus by CRISPR mediated knock-in. (H) RT-qPCR in $blanks^{KG00084}$/Df for *kl-3* using the indicated primer sets. Primer locations are designated by red bars on the gene diagram. Data was normalized to GAPDH and sibling controls. Mean ±SD (p-value $^{***}\leq 0.001$ t-test between mutant and control siblings, exact p-values listed in S1 Dataset.

https://doi.org/10.1371/journal.pgen.1008028.g003

GAPDH and sibling controls (Fig 3H). We noted a detectable drop between the early primer sets (~75% reduction in expression levels compared to controls) and the middle/late primer sets (~95% reduction in expression levels compared to controls), raising the possibility that *blanks* mutants may have difficulty transcribing this Y-loop gene soon after encountering the first satellite DNA-containing gigantic intron or stabilizing *kl-3* transcripts. A recent study that examined global expression changes in *blanks* mutant testes reported a similar change in *kl-3* gene expression [67]. In summary, the RNA-binding protein Blanks localizes to Y-loop B and allows for the robust transcription of the Y-loop B gene *kl-3*.

In contrast to Y-loop B/*kl-3* expression, Y-loop A/*kl-5* expression appeared normal in *blanks* mutants. We designed RNA FISH probes against *kl-5* in the same manner as for *kl-3* (i.e. early exon, intron and late exon) (Fig 4A, S1 File). We found that transcription of Y-loop A/*kl-5* follows a spatiotemporal pattern similar to that of Y-loop B/*kl-3* (Fig 4B and 4C): early exon transcripts become detectable in early SCs while *kl-5* mRNA granules are not detected in the cytoplasm until near the end of SC development (Fig 4B and 4C). No overt differences are observed in *kl-5* expression in *blanks* mutants and *kl-5* mRNA granules are observed in the cytoplasm (Fig 4D and 4E). By RT-qPCR with primers for *kl-5* designed similarly as described above for *kl-3* (Fig 3H), we found a mild reduction in *kl-5* expression in *blanks* mutants when normalized to GAPDH and sibling controls (Fig 4F). However, considering the fact that the *kl-5* mRNA granule is correctly formed in *blanks* mutant testes (Fig 4E), this reduction may not be biologically significant. The mild reduction in *kl-5* transcript in *blanks* mutants could be an indirect effect caused by defective Y-loop B expression. Alternatively, it is possible that a small amount of $(AATAT)_n$ satellite, which is predicted to be present in the last intron of *kl-5* [43, 68], might cause this mild reduction in *kl-5* expression in *blanks* mutant testes.

Blanks is unlikely to be a part of the general meiotic transcription program

It is well known that SCs utilize a specialized transcription program in order to transcribe the vast majority of genes required for meiosis and spermiogenesis [28, 69, 70]. This program is executed by two groups of transcription factors: tMAC and the tTAFs. The tMAC (testis-specific meiotic arrest complex) complex has both activating and repressing activities and has been shown to physically interact with the core transcription initiation machinery [71–77]. The tTAFs (testis-specific TATA binding protein associated factors) are homologs of core transcription initiation factors [78–81]. tMAC and the tTAFs function cooperatively to regulate meiotic gene expression. To examine whether *blanks* is part of this established meiotic transcription program, we examined the expression of *fzo* and *Dic61B*, known targets of the SC-specific transcriptional program [70, 79], which are located on autosomes and do not have gigantic introns (S1 File). In contrast to mutants for the tMAC component *aly* ($aly^{2/5P}$), which has drastically reduced levels of *fzo* and *Dic61B* transcripts, the expression of these genes is not visibly affected in *blanks* mutants (S2 Fig), suggesting that *blanks* is not a part of the SC-specific transcriptional program involving tTAFs and tMAC. Instead, *blanks* is likely uniquely involved in the expression of the Y-loop genes.

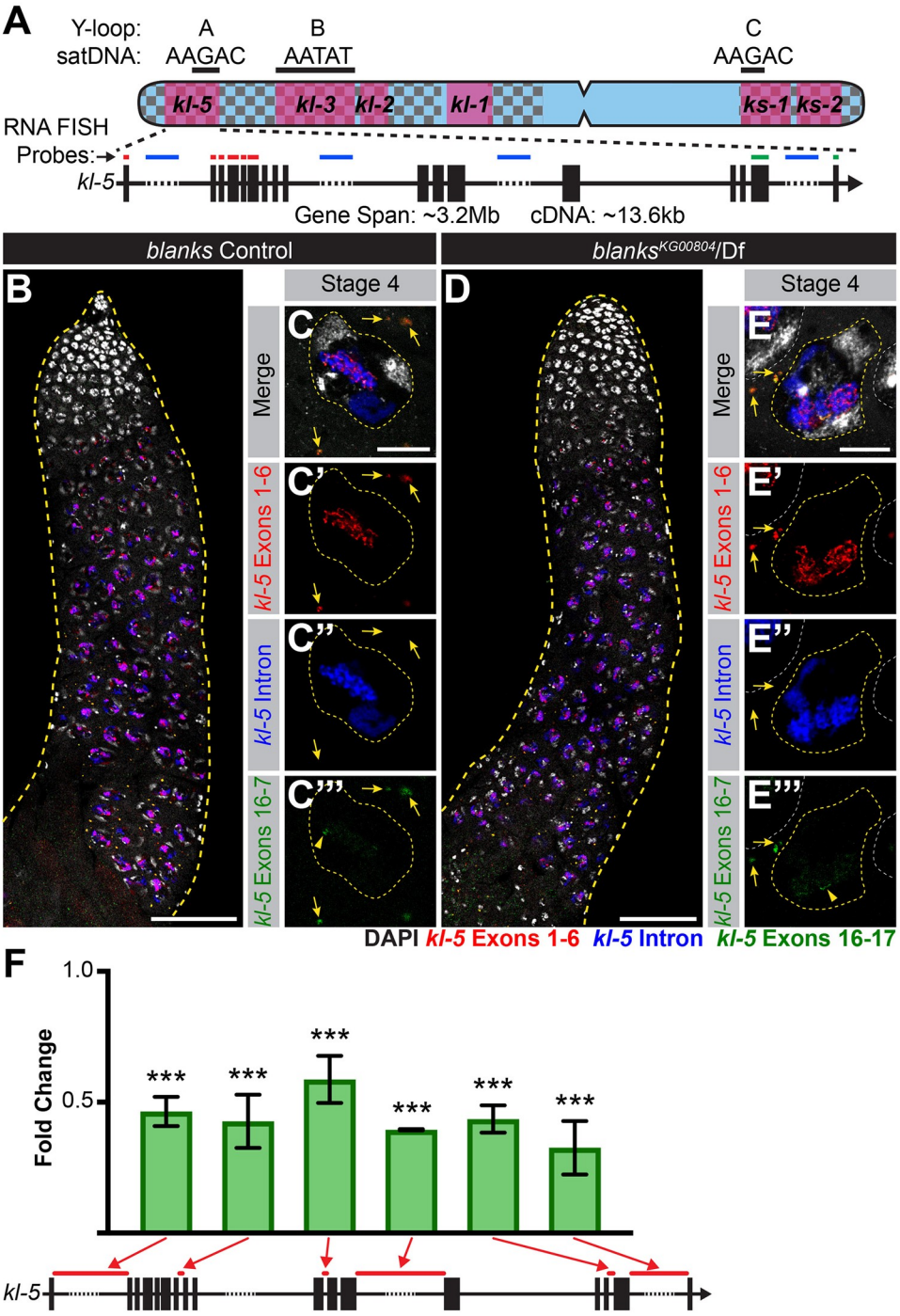

Fig 4. *blanks* is not required for *kl-5* expression. (A) Diagram of the Y-loop A gene *kl-5*. Exons (vertical rectangles), introns (black line) and intronic satellite DNA repeats (dashed line). Regions of *kl-5* targeted by RNA FISH probes are indicated by the colored bars. (B-E) RNA FISH against *kl-5* in *blanks* controls (B, C) and $blanks^{KG00084}$/Df (D, E). Exons 1–6 (red), *kl-5* intron ($Cy5\text{-}(AAGAC)_6$, blue), Exons 16–17 (green, arrowhead indicates nuclear signal), DAPI (white). (B, D) Apical third of the testis through the end of SC development (yellow dashed line). Bar: 75μm. (C, E) Single late SC nucleus (yellow dashed line). Nuclei of neighboring cells (white dashed line) and mRNA granules (yellow arrows). Bar: 10μm. (F) RT-qPCR in $blanks^{KG00084}$/Df for *kl-5* using the indicated primer sets. Primer locations are designated by red bars on the gene diagram. Data was normalized to GAPDH and sibling controls. Mean ±SD (p-value $^{***}\leq 0.001$, t-test between mutant and control siblings, exact p-values listed in S2 Dataset).

https://doi.org/10.1371/journal.pgen.1008028.g004

Heph is required for processing transcripts of the Y-loop A gene *kl-5*

As Heph-GFP localized to Y-loops A and C, we first examined whether Y-loops A and C displayed any overt expression defects in *heph* mutants (Fig 3B). When we performed RNA FISH to visualize the Y-loop gene intronic transcripts in *heph* mutants, the overall expression levels of both $(AAGAC)_n$ and $(AATAT)_n$ satellites appear unchanged between control and *heph* mutant testes (Fig 5A and 5B). However, we noted that the morphology of Y-loops A and C is altered in *heph* mutants, adopting a less organized, diffuse appearance (Fig 5B), whereas all Y-loops in control SCs show characteristic thread-like or globular morphologies (Fig 5A). Y-loop B appears unchanged between controls and *heph* mutants (Fig 5A and 5B). These results indicate that *heph* may be important for structurally organizing Y-loop A and C transcripts, without affecting overall transcript levels.

We next examined the expression pattern of *kl-5* exons together with the Y-loop A/C intronic satellite $[(AAGAC)_n]$, as described in Fig 4. Overall expression levels of *kl-5* appear to be unaltered in *heph* mutant testes (Fig 5C and 5E). However, in contrast to control testes (Fig 5D), *heph* mutant testes rarely have cytoplasmic *kl-5* mRNA granules in late SCs (Fig 5F), suggesting that *heph* mutants affect *kl-5* mRNA production without affecting transcription in the nucleus. *heph* mutants may be defective in processing the long repetitive regions of transcripts to generate mRNA (e.g. splicing, mRNA export or protection from degradation). We also examined the expression of *ks-1* (*ORY*) in *heph* mutants as Heph-GFP also localized to Y-loop C. While the *ORY* ORF is too short to allow for designing exon-specific probes to examine temporal expression patterns, RNA FISH with probes targeting all exons of *ORY* revealed that *ORY* mRNA granules are not formed in *heph* mutants (S3 Fig). Similar to *blanks* mutants, *heph* mutants show no defects in the expression of *fzo* or *Dic61B* (S2 Fig), indicating that *heph* is not a member of the more general meiotic transcription program. Instead, *heph*, like *blanks*, appears to specifically affect the expression of Y-loops to which it localizes.

RT-qPCR showed that *heph* mutants only exhibit a moderate reduction in *kl-5* expression when normalized to GAPDH and sibling controls (Fig 5G), which is in accordance with the RNA FISH results described above. A similar moderate reduction in *kl-5* mRNA is observed in *blanks* mutants (Fig 4F), which do not affect *kl-5* mRNA granule formation. Thus, it is unlikely that the reduction in *kl-5* expression levels alone causes the lack of *kl-5* mRNA granules in *heph* mutant SCs. Instead, we postulate that mRNA granule formation is dependent on proper processing or stability of primary transcripts, which may be defective in *heph* mutants.

Surprisingly, we found that *kl-3* mRNA granules are also absent in *heph* mutants, although Y-loop B/*kl-3* expression levels in the nucleus appear to be unaffected (Fig 6A–6D). RT-qPCR showed a similar moderate reduction in *kl-3* mRNA in *heph* mutants when normalized to GAPDH and sibling controls (Fig 6E) as was observed in *kl-5* mRNA (Fig 5G). Consistent with the absence of cytoplasmic *kl-3* mRNA granules, Kl-3 protein levels are dramatically reduced in *heph* mutant testes (Fig 6F). This is unexpected as Heph protein does not localize to Y-loop B (Fig 2B) or affect Y-loop B morphology (Fig 5A and 5B). It is possible that some of the predicted 25 isoforms of Heph are not visualized by Heph-GFP, and these un-visualized isoforms might localize to and regulate Y-loop B/*kl-3* expression. Alternatively, this may be an indirect effect of defective Y-loop A and C expression and/or structure.

Taken together, our results show that Blanks and Heph, two RNA-binding proteins, are essential for the expression of Y-loop genes, but are not members of the more general meiotic transcription program. As Y-loop genes are essential for sperm motility and fertility, the sterility observed in *blanks* and *heph* mutants likely stems from defects in Y-loop gene expression. Blanks and Heph highlight two distinct steps (transcriptional processivity and RNA processing (e.g. splicing, export and/or stability of transcripts)) in a unique Y-loop gene expression program.

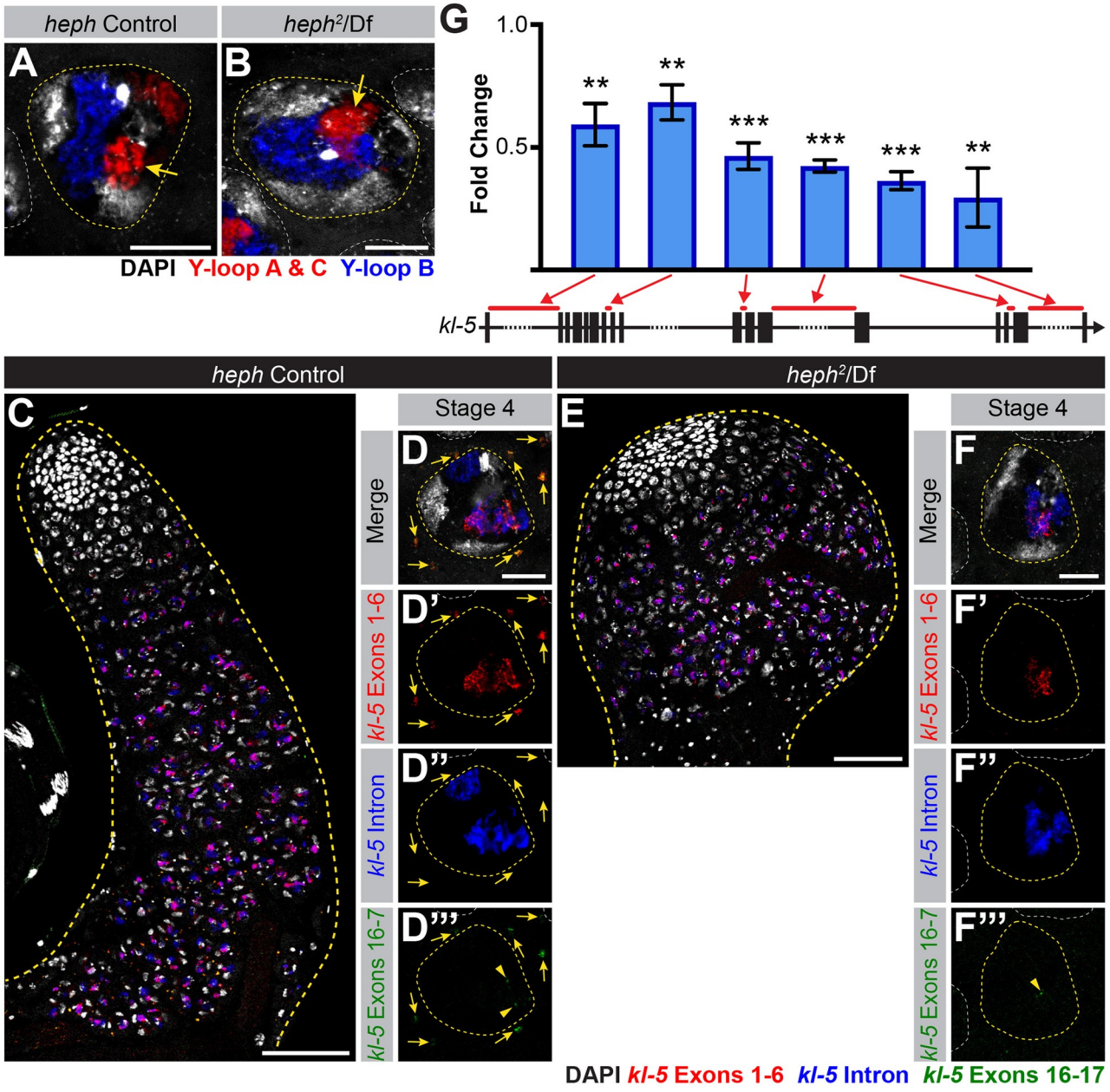

Fig 5. *kl-5* mRNA granules are absent in *heph* mutants. (A, B) RNA FISH against the Y-loop gene intronic transcripts in *heph* controls (A) and *heph*^{2}/Df (B). Single late SC nuclei (yellow dashed line), nuclei of neighboring cells (white dashed line), Y-loops A and C (Cy3-$(AAGAC)_6$, red), Y-loop B (Cy5-$(AATAT)_6$, blue) and DAPI (white). Bar: 10μm. (C-F) RNA FISH against *kl-5* in *heph* controls (C, D) and *heph*^{2}/Df (E, F). Exons 1–6 (red), *kl-5* intron (Cy5-$(AAGAC)_6$, blue), Exons 16–17 (green, arrowhead indicates nuclear signal) and DAPI (white). (C, E) Apical third of the testis through the end of SC development (yellow dashed line). The bulbous shape of *heph*^{2}/Df is a known phenotype that can occur with this allele [62]. Bar: 75μm. (D, F) Single late SC nuclei (yellow dashed line). Nuclei of neighboring cells (white dashed line) and mRNA granules (yellow arrows). Bar: 10μm. (G) RT-qPCR in *heph*^{2}/Df for *kl-5* using the indicated primer sets. Primer locations are designated by red bars on the gene diagrams. Data was normalized to GAPDH and sibling controls. Mean ±SD (p-value $^{**}\leq 0.01$, $^{***}\leq 0.001$, t-test between mutant and control siblings, exact p-values listed in S3 Dataset).

https://doi.org/10.1371/journal.pgen.1008028.g005

Discussion

The existence of the Y chromosome lampbrush-like loops of *Drosophila* has been known for the last five decades [82, 83], however little is known as to how Y-loop formation and

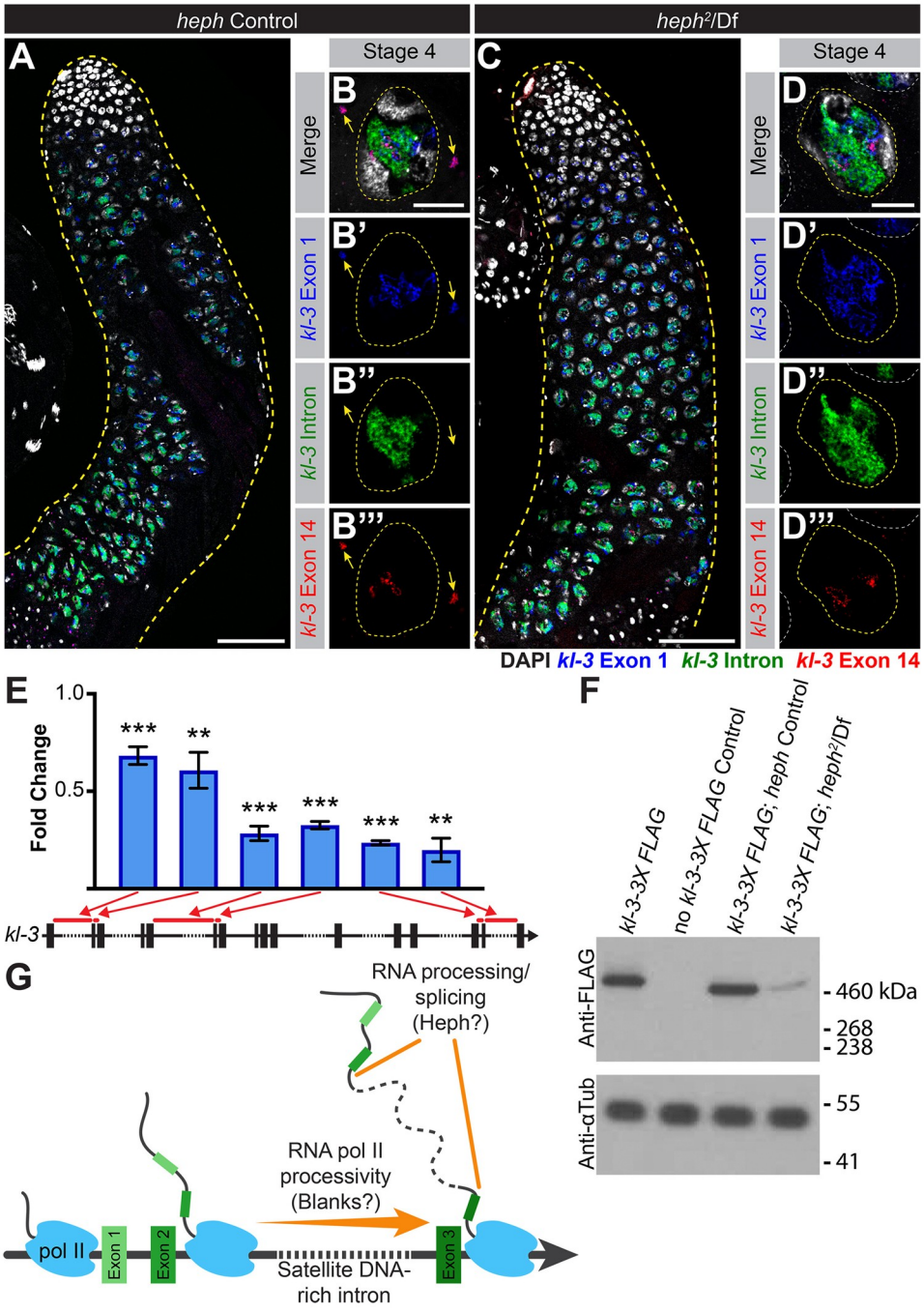

Fig 6. *kl-3* expression is affected in *heph* mutants. (A—D) RNA FISH against *kl-3* in *heph* controls (A, B) and *heph*^{2}/Df (C, D). Exon 1 (blue), *kl-3* intron (Alexa488-$(AATAT)_6$, green), Exon 14 (red) and DAPI (white). (A, C) Apical third of the testis through the end of SC development (yellow dashed line). Bar: 75μm. (B, D) Single late SC nuclei (yellow dashed line). Nuclei of neighboring cells (white dashed line) and mRNA granules (yellow arrows). Bar: 10μm. (E) RT-qPCR in *heph*^{2}/Df for *kl-3* using the indicated primer sets. Primer locations are designated by red bars on the gene diagrams. Data was normalized to GAPDH and sibling controls. Mean ±SD (p-value $^{**}\leq 0.01$, $^{***}\leq 0.001$, t-test between mutant and control siblings, exact p-values listed in S4 Dataset). (F) Western blot for Kl-3-3X FLAG in the indicated genotypes. (G) Model for the Y-loop gene expression program.

https://doi.org/10.1371/journal.pgen.1008028.g006

expression is regulated and whether these SC-specific structures are important for spermatogenesis. Here we identified a Y-loop gene-specific expression program that functions in parallel to the general meiotic transcriptional program to aid in the expression and processing of the gigantic Y-loop genes. Our results suggest that genes with intron gigantism, such as the Y-loop genes and potentially other large genes such as Dystrophin, require specialized mechanisms for proper expression.

The mutant phenotypes of *blanks* and *heph*, the two genes identified to be involved in this novel expression program, highlight two distinct steps of the Y-loop gene specific expression program (Fig 6G). Blanks was originally identified as an siRNA binding protein, but no defects in small RNA mediated silencing were observed in the testes of *blanks* mutants [55, 56]. We found that *blanks* is required for transcription of Y-loop B/*kl-3*, as nuclear transcript levels were visibly reduced in *blanks* mutants, leading to the lack of both *kl-3* mRNA granules in the cytoplasm and Kl-3 protein. As Blanks' ability to bind RNA was previously found to be required for male fertility [55], we speculate that Blanks may bind to newly synthesized nascent *kl-3* RNA, which contain megabases of satellite DNA transcripts, so that transcripts' secondary/tertiary structures do not interfere with transcription [84]. It is possible that elongating RNA polymerases, which slow and potentially lose stability on repetitive DNAs [46, 49], might require Blanks to increase processivity, allowing them to transcribe through repetitive DNA sequences, as has been observed for repetitive sequences in other systems [85–87].

Heph has been implicated in a number of steps in RNA processing and translational regulation [88–91], but Heph's exact role in the testis remained unclear despite its requirement for male fertility [60, 61]. We found that *heph* mutants fail to generate *kl-5* cytoplasmic mRNA granules even though nuclear transcript levels appeared minimally affected. This suggests that *heph* may be required for processing the long repetitive transcripts. For example, *heph* might be required to ensure proper splicing of the Y-loop gene pre-mRNAs, which is predicted to be challenging as the splicing of adjacent exons becomes exponentially more difficult as intron length increases [92]. Y-loop genes may utilize proteins like Heph to combat this challenge or alternatively, Heph could aid in stabilizing this long RNA and preventing premature degradation.

These results highlight the presence of a unique program tailored toward expressing genes with intron gigantism. Although the functional relevance of intron gigantism remains obscure, our results may provide hints as to the possible functions of intron gigantism. Even if intron gigantism did not arise to serve a specific function, once it emerges, the unique gene expression program that can handle intron gigantism must evolve to tolerate the burden of gigantic introns, as indicated by our study on *blanks* and *heph* mutants. Ultimately, the presence of a unique gene expression program for genes with gigantic introns would provide a unique opportunity to regulate gene expression. Once such systems evolve, other or new genes may start utilizing such a gene expression program to add an additional layer of complexity to the regulation of gene expression. For example, in the case of Y-loop genes, the extended time period required for the transcription of the gigantic Y-loop genes (~80–90 hours) might function as a 'developmental timer' for SC differentiation. Similar to this idea, it was shown that the expression of two homologous genes, *knirps* (*kni*) and *knirps-like* (*knrl*), is regulated by intron size during embryogenesis in *Drosophila*. Although *knrl* can perform the same function as *kni* in embryos, mRNA of *knrl* is not produced due to the presence of a relatively large (14.9kb) intron (as opposed to the small (<1kb) introns of *kni*), which prevents completion of *knrl* transcription during the short cell cycles of early development [93]. A similar idea was proposed for *Ultrabithorax* (*Ubx*) in the early *Drosophila* embryo, where large gene size led to abortion of transcription of *Ubx* during the syncytial divisions of *Drosophila* embryos, preventing production of Ubx protein. [94]. Thus, intron size can play a critical role in the regulation

of gene expression. Alternatively, satellite DNA-containing gigantic introns could act in a manner similar to enhancers, recruiting transcriptional machinery to the Y-loop genes to facilitate expression [1].

In summary, our study provides the first glimpse at how the expression of genes with intron gigantism requires a unique gene expression program, which acts on both transcription and post-transcriptional processing.

Materials and methods

Fly Husbandry

All fly stocks were raised on standard Bloomington medium at 25˚C, and young flies (1- to 3-day-old adults) were used for all experiments. Flies used for wild-type experiments were the standard lab wild-type strain *yw* (y^1w^1). The following fly stocks were used: $heph^2$ (BDSC:635), Df(3R)BSC687 (BDSC: 26539), $blanks^{KG00084}$ (BDSC:13914), Df(3L)BSC371 (BDSC:24395), p(PTT-GC)$heph^{CC00664}$ (BDSC:51540), $UAS\text{-}kl\text{-}3^{TRiP.HMC03546}$ (BDSC:53317), $UAS\text{-}blanks^{TRiP.HMS00078}$ (BDSC:33667), $UAS\text{-}kl\text{-}5^{TRiP.HMC03747}$ (BDSC:55609), and C(1)RM/C(1;Y)6, $y^1w^1f^1$/0 (BDSC:9460) were obtained from the Bloomington Stock Center (BDSC). *GFP-blanks* (GFP-tagged Blanks expressed by it's endogenous promoter) was a gift of Dean Smith [55]. *bam-gal4* was a gift of Dennis McKearin [95]. The aly^2 and aly^{5P} stocks were a gift of Minx Fuller [69].

It is important to note that the $heph^2$ allele is known to be male sterile whereas other *heph* alleles are lethal, thus the $heph^2$ allele is unlikely to be null and affects only a subset of isoforms, including one/those with a testis-specific function. The Y chromosome in the *heph* deficiency strain Df(3R)BSC687 appeared to have accumulated mutations that resulted in abnormal Y-loop morphology. This Y chromosome was replaced with the *yw* Y chromosome for all experiments described in this study.

The *kl-3-FLAG* strain was constructed by Fungene (fgbiotech.com) using CRISPR mediated knock-in of a 3X-FLAG tag in frame at the endogenous C-terminus immediately preceding the termination codon of *kl-3* using homology-directed repair. Two guide RNAs were used (CCACTGGACTTTAAGGGGTGTTGC and GCATCCTGACCACTGGACTTTAAG) and point mutations were introduced in the PAM sequences following homology directed repair to prevent continued cutting.

RNA Fluorescent *in situ* hybridization

All solutions used for RNA FISH were RNase free. Testes from 2–3 day old flies were dissected in 1X PBS and fixed in 4% formaldehyde in 1X PBS for 30 minutes. Then testes were washed briefly in PBS and permeabilized in 70% ethanol overnight at 4˚C. Testes were briefly rinsed with wash buffer (2X saline-sodium citrate (SSC), 10% formamide) and then hybridized overnight at 37˚C in hybridization buffer (2X SSC, 10% dextran sulfate (sigma, D8906), 1mg/mL E. coli tRNA (sigma, R8759), 2mM Vanadyl Ribonucleoside complex (NEB S142), 0.5% BSA (Ambion, AM2618), 10% formamide). Following hybridization, samples were washed three times in wash buffer for 20 minutes each at 37˚C and mounted in VECTASHIELD with DAPI (Vector Labs). Images were acquired using an upright Leica TCS SP8 confocal microscope with a 63X oil immersion objective lens (NA = 1.4) and processed using Adobe Photoshop and ImageJ software.

Fluorescently labeled probes were added to the hybridization buffer to a final concentration of 50nM (for satellite DNA transcript targeted probes) or 100nM (for exon targeted probes). Probes against the satellite DNA transcripts were from Integrated DNA Technologies. Probes against *kl-3*, *kl-5*, *fzo*, and *Dic61B* exons were designed using the Stellaris® RNA FISH Probe

Designer (Biosearch Technologies, Inc.) available online at www.biosearchtech.com/stellarisdesigner. Each set of custom Stellaris® RNA FISH probes was labeled with Quasar 670, Quasar 570 or Fluorescein-C3 (S1 File).

For strains expressing GFP (e.g. GFP-Blanks, Heph-GFP), the overnight permeabilization in 70% ethanol was omitted.

RT-qPCR

Total RNA from testes (50 pairs/sample) was extracted using TRIzol (Invitrogen) according to the manufacturer's instructions. 1μg of total RNA was reverse transcribed using SuperScript III® Reverse Transcriptase (Invitrogen) followed by qPCR using *Power* SYBR Green reagent (Applied Biosystems). Primers for qPCR were designed to amplify only mRNA. For average introns, one primer of the pair was designed to span the two adjacent exons. Primers spanning large introns could only produce a PCR product if the intron has been spliced out. Relative expression levels were normalized to GAPDH and control siblings. All reactions were done in technical triplicates with at least two biological replicates. Graphical representation was inclusive of all replicates and p-values were calculated using a t-test performed on untransformed average ddct values. Primers used are listed in S3 File.

Western blot

Testes (40 pairs/sample) were dissected in Schneider's media at room temperature within 30 minutes, the media was removed and the samples were frozen at -80˚C until use. After thawing, testes were then lysed in 200uL of 2X Laemmli Sample Buffer + βME (BioRad, 161–0737). Samples were separated on a NuPAGE Tris-Acetate gel (3–8%, 1.5mm, Invitrogen) and transferred onto polyvinylidene fluoride (PVDF) membrane (Immobilon-P, Millipore) using NuPAGE transfer buffer (Invitrogen) without added methanol. Membranes were blocked in 1X TBST (0.1% Tween-20) containing 5% nonfat milk, followed by incubation with primary antibodies diluted in 1X TBST containing 5% nonfat milk. Membranes were washed with 1X TBST, followed by incubation with secondary antibodies diluted in 1X TBST containing 5% nonfat milk. After washing with 1X TBST, detection was performed using the Pierce® ECL Western Blotting Substrate enhanced chemiluminescence system (Thermo Scientific). Primary antibodies used were anti–α-tubulin (1:2,000; mouse, monoclonal, clone DM1a; Sigma-Aldrich) and anti-FLAG (1:2,500; mouse, monoclonal, M2, Sigma-Aldrich). The secondary antibody was horseradish peroxidase (HRP) conjugated anti-mouse IgG (1:10,000; Jackson ImmunoResearch Laboratories).

Screen for the identification of proteins involved in Y-loop gene expression

Initially, ~2200 candidate genes were selected based on gene ontology (GO) terms (e.g.. "mRNA binding", "regulation of translation", "spermatid development"). These genes were cross-referenced against publicly available RNAseq data sets (i.e.: FlyAtlas, modENCODE) and only those genes predicted to be expressed in the testis were selected. Additionally, candidate genes were eliminated if they are known to be involved in ubiquitous processes (e.g. general transcription factors, ribosomal subunits) or processes that are seemingly unrelated to those associated with the Y-loop genes (e.g. mitochondrial proteins, GSC/SG differentiation, mitotic spindle assembly). Finally, candidates were limited to those with available reagents for localization and/or phenotypic analysis, leaving a final list of 67 candidate genes (S2 File). If available, we first analyzed protein localization for each candidate. If candidate proteins did not localize to SCs or the Y-loops, they were not further examined. If the candidate was found to be expressed in SCs or if no localization reagents were available, then RNAi mediated

knockdown or mutants were used to examine Y-loop gene expression for any deviations from the expression pattern described in Fig 1D–1H and to assess fertility. As Y-loop genes are all essential for sperm maturation [14], any genes essential for Y-loop gene expression should also be needed for fertility. All selection criteria and a summary of phenotypes observed can be found in S2 File.

Phalloidin staining

Testes were dissected in 1X PBS, transferred to 4% formaldehyde in 1X PBS and fixed for 30 minutes. Testes were then washed in 1X PBST (PBS containing 0.1% Triton-X) for at least 60 minutes followed by incubation with Phalloidin-Alexa546 (ThermoFisher, a22283, 1:200) antibody in 3% bovine serum albumin (BSA) in 1X PBST at 4˚C overnight. Samples were washed for 60 minutes in 1X PBST and mounted in VECTASHIELD with DAPI (Vector Labs). Images were acquired using an upright Leica TCS SP8 confocal microscope with a 63X oil immersion objective lens (NA = 1.4) and processed using Adobe Photoshop and ImageJ software.

Seminal vesicle imaging and analysis

To determine the presence of motile sperm, testes with seminal vesicles were dissected in 1X PBS, transferred to 4% formaldehyde in 1X PBS and fixed for 30 minutes. Testes were then washed in 1X PBST (PBS containing 0.1% Triton-X) for at least 60 minutes and mounted in VECTASHIELD with DAPI (Vector Labs). Seminal vesicles were then examined by confocal microscopy. The number of sperm nuclei, as determined by DAPI staining, was observed. If comparable to wildtype, the seminal vesicle was scored as having a normal number of motile sperm, if the seminal vesicle contained no detectable sperm nuclei, it was scored as empty and if the seminal vesicle contained only a few sperm, it was scored as greatly reduced.

To obtain representative images, seminal vesicles were dissected in 1X PBS and transferred to slides for live observation by phase contrast on a Leica DM5000B microscope with a 40X objective (NA = 0.75) and imaged with a QImaging Retiga 2000R Fast 1394 Mono Cooled camera. Images were adjusted in Adobe Photoshop.

Supporting information

S1 Fig. *blanks* RNAi recapitulates the phenotypes observed in *blanks* mutants. (A) RNA FISH against the Y-loop gene intronic transcripts in *bam-gal4>UAS-blanks*$^{TRiP.HMS00078}$ testes. Testis outline (yellow dashed line), Y-loops A and C (Cy3-$(AAGAC)_6$, red), Y-loop B (Cy5-$(AATAT)_6$, blue) and DAPI (white). Comparable stage SC (yellow arrow, compare to Fig 3A and 3B). Bar: 50μm. High magnification image of a single SC at a comparable stage (compare to Fig 3A and 3B) is provided below. SC nucleus (yellow dashed line) and nuclei of neighboring cells (white dashed line). Bar: 10μm. (B, C) RNA FISH against *kl-3* in *bam-gal4>UAS-blanks*$^{TRiP.HMS00078}$ testes. Exon 1 (blue), *kl-3* intron (Alexa488-$(AATAT)_6$, green), Exon 14 (red) and DAPI (white). (B) Apical third of the testis through the end of SC development (yellow dashed line). Bar: 75μm. (C) Single late SC nucleus (yellow dashed line). Nuclei of neighboring cells (white dashed line) and mRNA granules (yellow arrows). Bar: 10μm.
(TIF)

S2 Fig. Blanks and Heph are not part of the meiotic transcriptional program. RNA FISH against *fzo* (A-E) and *Dic61B* (A'-E') in *blanks* controls (A), *blanks*^{KG00084}/Df (B), *heph* controls (C), *heph*^{2}/Df (D), and *aly*$^{2/5P}$ (E). Apical third of the testis through the end of SC development (yellow dashed line). DAPI (white). Bar: 75μm.
(TIF)

S3 Fig. Y-loop C/*ORY* expression is perturbed in *heph* mutants. RNA FISH against *ORY* in *heph* controls (A) and $heph^2$/Df (B). Exons (red), *ORY* intron ($Cy3\text{-}(AAGAC)_6$, blue), DAPI (white), single late SC nucleus (yellow dashed line), nuclei of neighboring cells (white dashed line) and mRNA granules (yellow arrows). Bar: 10μm.
(TIF)

S1 File. Probes for RNA FISH.
(DOCX)

S2 File. Screen summary.
(DOCX)

S3 File. RT-qPCR primers.
(DOCX)

S1 Dataset. Fold change calculations for *kl-3* in *blanks* mutants.
(XLSX)

S2 Dataset. Fold change calculations for *kl-5* in *blanks* mutants.
(XLSX)

S3 Dataset. Fold change calculations for *kl-5* in *heph* mutants.
(XLSX)

S4 Dataset. Fold change calculations for *kl-3* in *heph* mutants.
(XLSX)

Acknowledgments

We thank Dean Smith, Dennis McKearin, Minx Fuller and the Bloomington Stock Center for reagents. We thank the Yamashita laboratory and Drs. Sue Hammoud and Lei Lei for discussions and comments on the manuscript, Dr. Ruth Lehmann for helpful suggestions and Dr. Jiandie Lin for sharing equipment.

Author Contributions

Conceptualization: Jaclyn M. Fingerhut, Yukiko M. Yamashita.

Formal analysis: Jaclyn M. Fingerhut, Yukiko M. Yamashita.

Funding acquisition: Yukiko M. Yamashita.

Investigation: Jaclyn M. Fingerhut, Jessica V. Moran, Yukiko M. Yamashita.

Supervision: Yukiko M. Yamashita.

Writing – original draft: Jaclyn M. Fingerhut, Yukiko M. Yamashita.

Writing – review & editing: Jaclyn M. Fingerhut, Yukiko M. Yamashita.

References

1. Shaul O. How introns enhance gene expression. Int J Biochem Cell Biol. 2017; 91(Pt B):145–55. https://doi.org/10.1016/j.biocel.2017.06.016 PMID: 28673892.
2. Scherer S. Guide to the human genome. Cold Spring Harbor, N.Y.: Cold Spring Harbor Laboratory Press; 2010. xiv, 1008 p. p.
3. Pozzoli U, Sironi M, Cagliani R, Comi GP, Bardoni A, Bresolin N. Comparative analysis of the human dystrophin and utrophin gene structures. Genetics. 2002; 160(2):793–8. PMID: 11861579

4. Pozzoli U, Elgar G, Cagliani R, Riva L, Comi GP, Bresolin N, et al. Comparative analysis of vertebrate dystrophin loci indicate intron gigantism as a common feature. Genome Res. 2003; 13(5):764–72. https://doi.org/10.1101/gr.776503 PMID: 12727896
5. Lohe AR, Hilliker AJ, Roberts PA. Mapping simple repeated DNA sequences in heterochromatin of Drosophila melanogaster. Genetics. 1993; 134(4):1149–74. PMID: 8375654
6. Hoskins RA, Smith CD, Carlson JW, Carvalho AB, Halpern A, Kaminker JS, et al. Heterochromatic sequences in a Drosophila whole-genome shotgun assembly. Genome Biol. 2002; 3(12): RESEARCH0085. https://doi.org/10.1186/gb-2002-3-12-research0085 PMID: 12537574
7. Carvalho AB. Origin and evolution of the Drosophila Y chromosome. Current opinion in genetics & development. 2002; 12(6):664–8. Epub 2002/11/16. PMID: 12433579.
8. Peacock WJ, Lohe AR, Gerlach WL, Dunsmuir P, Dennis ES, Appels R. Fine structure and evolution of DNA in heterochromatin. Cold Spring Harb Symp Quant Biol. 1978; 42 Pt 2:1121–35. PMID: 98264.
9. Carvalho AB, Vicoso B, Russo CAM, Swenor B, Clark AG. Birth of a new gene on the Y chromosome ofDrosophila melanogaster. Proceedings of the National Academy of Sciences. 2015; 112(40):12450–5. https://doi.org/10.1073/pnas.1516543112 PMID: 26385968
10. Brosseau GE. Genetic Analysis of the Male Fertility Factors on the Y Chromosome of Drosophila Melanogaster. Genetics. 1960; 45(3):257–74. PMID: 17247923
11. Gatti M, P S. Cytological and genetic analysis of the Y chromosome of *Drosophila melanogaster*. Chromosoma. 1983; 88:349–73. https://doi.org/10.1007/BF00285858
12. Hazelrigg T, F P., Kaufman T.C. A Cytogenetic Analysis of X-ray Induced Male Steriles on the Y Chromosome of *Drosophila melanogaster*. Chromosoma. 1982; 87:535–59.
13. Kennison JA. The Genetic and Cytological Organization of the Y Chromosome of *Drosophila melanogaster*. Genetics. 1981; 98(3):529–48. PMID: 17249098
14. Hardy RW, Tokuyasu KT, Lindsley DL. Analysis of spermatogenesis in Drosophila melanogaster bearing deletions for Y-chromosome fertility genes. Chromosoma. 1981; 83(5):593–617. PMID: 6794995.
15. Goldstein LS, Hardy RW, Lindsley DL. Structural genes on the Y chromosome of Drosophila melanogaster. Proc Natl Acad Sci U S A. 1982; 79(23):7405–9. PMID: 6818544
16. Carvalho AB, Lazzaro BP, Clark AG. Y chromosomal fertility factors kl-2 and kl-3 of Drosophila melanogaster encode dynein heavy chain polypeptides. Proc Natl Acad Sci U S A. 2000; 97(24):13239–44. https://doi.org/10.1073/pnas.230438397 PMID: 11069293
17. Bonaccorsi S, Pisano C, Puoti F, Gatti M. Y chromosome loops in Drosophila melanogaster. Genetics. 1988; 120(4):1015–34. PMID: 2465201
18. Pimpinelli S, B S., Gatti M., Sandler L. The peculiar genetic organization of *Drosophila* heterochromatin. Trends in Genetics. 1986; 2:17–20.
19. Marsh JL, Wieschaus E. Is sex determination in germ line and soma controlled by separate genetic mechanisms? Nature. 1978; 272(5650):249–51. PMID: 628449.
20. Bridges CB. Non-Disjunction as Proof of the Chromosome Theory of Heredity. Genetics. 1916; 1(1):1–52. PMID: 17245850
21. Yamashita YM. Subcellular Specialization and Organelle Behavior in Germ Cells. Genetics. 2018; 208 (1):19–51. https://doi.org/10.1534/genetics.117.300184 PMID: 29301947
22. Chandley AC, Bateman AJ. Timing of spermatogenesis in Drosophila melanogaster using tritiated thymidine. Nature. 1962; 193:299–300. PMID: 13878048.
23. Fuller MT. Spermatogenesis. In: Bate M, Arias A.M., editor. The Development of Drosophila Melanogaster. 1. New York: Cold Spring Harbor Laboratory Press; 1993. p. 71–148.
24. McKee BD, Yan R, Tsai JH. Meiosis in male Drosophila. Spermatogenesis. 2012; 2(3):167–84. https://doi.org/10.4161/spmg.21800 PMID: 23087836
25. Schafer M, Nayernia K, Engel W, Schafer U. Translational control in spermatogenesis. Dev Biol. 1995; 172(2):344–52. https://doi.org/10.1006/dbio.1995.8049 PMID: 8612956.
26. Olivieri G, Olivieri A. Autoradiographic study of nucleic acid synthesis during spermatogenesis in Drosophila melanogaster. Mutat Res. 1965; 2(4):366–80. PMID: 5878312.
27. Gould-Somero M, Holland L. The timing of RNA synthesis for spermiogenesis in organ cultures ofDrosophila melanogaster testes. Wilhelm Roux Arch Entwickl Mech Org. 1974; 174(2):133–48. https://doi.org/10.1007/BF00573626 PMID: 28305043.
28. White-Cooper H, Caporilli S. Transcriptional and post-transcriptional regulation of Drosophila germline stem cells and their differentiating progeny. Adv Exp Med Biol. 2013; 786:47–61. https://doi.org/10.1007/978-94-007-6621-1_4 PMID: 23696351.

29. Piergentili R. Evolutionary conservation of lampbrush-like loops in drosophilids. BMC Cell Biol. 2007; 8:35. https://doi.org/10.1186/1471-2121-8-35 PMID: 17697358

30. Hess O. [Morphologic variability of chromosomal functional structures in spermatocyte nuclei of Drosophila species]. Chromosoma. 1967; 21(4):429–45. PMID: 4861894.

31. Hackstein JH, Leoncini O, Beck H, Peelen G, Hennig W. Genetic fine structure of the Y chromosome of Drosophila hydei. Genetics. 1982; 101(2):257–77. PMID: 7173604

32. Wlaschek M, Awgulewitsch A, Bunemann H. Structure and function of Y chromosomal DNA. I. Sequence organization and localization of four families of repetitive DNA on the Y chromosome of Drosophila hydei. Chromosoma. 1988; 96(2):145–58. PMID: 3349874.

33. Vogt P, H W. Molecular structure of the lampbrush loops nooses of the Y chromosome of Drosophila hydei: II. DNA sequences with homologies to multiple gemonic locations are major constituents of the loop. Chromosoma. 1986; 94:459–67.

34. Vogt P, H W. Molecular structure of the lampbrush loops nooses of the Y chromosome of *Drosophila hydei*: I. The Y chromosome-specific repetitive DNA sequence family ay1 is dispersed in the loop DNA. Chromosoma. 1986; 94:449–58.

35. Trapitz P, Glatzer KH, Bunemann H. Towards a physical map of the fertility genes on the heterochromatic Y chromosome of Drosophila hydei: families of repetitive sequences transcribed on the lampbrush loops Nooses and Threads are organized in extended clusters of several hundred kilobases. Mol Gen Genet. 1992; 235(2–3):221–34. PMID: 1465096.

36. Huijser P, Beckers L, Top B, Hermans M, Sinke R, Hennig W. Poly[d(C-A)].poly[d(G-T)] is highly transcribed in the testes of Drosophila hydei. Chromosoma. 1990; 100(1):48–55. PMID: 2129287.

37. Hochstenbach R, Brand R, Hennig W. Transcription of repetitive DNA sequences in the lampbrush loop pair Nooses formed by sterile alleles of fertility gene Q on the Y chromosome of Drosophila hydei. Mol Gen Genet. 1994; 244(6):653–60. PMID: 7969035.

38. Chang CH, Larracuente AM. Genomic changes following the reversal of a Y chromosome to an autosome in Drosophila pseudoobscura. Evolution. 2017; 71(5):1285–96. https://doi.org/10.1111/evo.13229 PMID: 28322435

39. Reugels AM, Kurek R, Lammermann U, Bunemann H. Mega-introns in the dynein gene DhDhc7(Y) on the heterochromatic Y chromosome give rise to the giant threads loops in primary spermatocytes of Drosophila hydei. Genetics. 2000; 154(2):759–69. PMID: 10655227

40. Kurek R, Trapitz P, Bunemann H. Strukturdifferenzierungen in Y-chromosom von Drosophila hydei: the unique morphology of the Y chromosomal lampbrush loops Threads results from 'coaxial shells' formed by different satellite-specific subregions within megabase-sized transcripts. Chromosome Res. 1996; 4(2):87–102. PMID: 8785614.

41. de Loos F, Dijkhof R, Grond CJ, Hennig W. Lampbrush chromosome loop-specificity of transcript morphology in spermatocyte nuclei of Drosophila hydei. EMBO J. 1984; 3(12):2845–9. PMID: 16453579

42. Grond CJ, S I., Hennig W. Visualization of a lampbrush loop-forming fertility gene in *Drosophila hydei*. Chromosoma. 1983; 88:50–6.

43. Bonaccorsi S, Lohe A. Fine mapping of satellite DNA sequences along the Y chromosome of Drosophila melanogaster: relationships between satellite sequences and fertility factors. Genetics. 1991; 129 (1):177–89. PMID: 1936957

44. Lasda EL, Blumenthal T. Trans-splicing. Wiley Interdiscip Rev RNA. 2011; 2(3):417–34. https://doi.org/10.1002/wrna.71 PMID: 21957027.

45. Dangkulwanich M, Ishibashi T, Bintu L, Bustamante C. Molecular mechanisms of transcription through single-molecule experiments. Chem Rev. 2014; 114(6):3203–23. https://doi.org/10.1021/cr400730x PMID: 24502198

46. Maiuri P, Knezevich A, De Marco A, Mazza D, Kula A, McNally JG, et al. Fast transcription rates of RNA polymerase II in human cells. EMBO Rep. 2011; 12(12):1280–5. https://doi.org/10.1038/embor.2011.196 PMID: 22015688

47. Li Y, Lu Y, Polak U, Lin K, Shen J, Farmer J, et al. Expanded GAA repeats impede transcription elongation through the FXN gene and induce transcriptional silencing that is restricted to the FXN locus. Hum Mol Genet. 2015; 24(24):6932–43. https://doi.org/10.1093/hmg/ddv397 PMID: 26401053

48. Kumari D, Biacsi RE, Usdin K. Repeat expansion affects both transcription initiation and elongation in friedreich ataxia cells. J Biol Chem. 2011; 286(6):4209–15. https://doi.org/10.1074/jbc.M110.194035 PMID: 21127046

49. Punga T, Buhler M. Long intronic GAA repeats causing Friedreich ataxia impede transcription elongation. EMBO Mol Med. 2010; 2(4):120–9. https://doi.org/10.1002/emmm.201000064 PMID: 20373285

50. Mason PB, Struhl K. Distinction and relationship between elongation rate and processivity of RNA polymerase II in vivo. Mol Cell. 2005; 17(6):831–40. https://doi.org/10.1016/j.molcel.2005.02.017 PMID: 15780939.

51. Cheng MH, Maines JZ, Wasserman SA. Biphasic subcellular localization of the DAZL-related protein boule in Drosophila spermatogenesis. Dev Biol. 1998; 204(2):567–76. https://doi.org/10.1006/dbio.1998.9098 PMID: 9882490.

52. Lowe N, Rees JS, Roote J, Ryder E, Armean IM, Johnson G, et al. Analysis of the expression patterns, subcellular localisations and interaction partners of Drosophila proteins using a pigP protein trap library. Development. 2014; 141(20):3994–4005. https://doi.org/10.1242/dev.111054 PMID: 25294943

53. Redhouse JL, Mozziconacci J, White RA. Co-transcriptional architecture in a Y loop in Drosophila melanogaster. Chromosoma. 2011; 120(4):399–407. https://doi.org/10.1007/s00412-011-0321-1 PMID: 21556802.

54. Heatwole VM, Haynes SR. Association of RB97D, an RRM protein required for male fertility, with a Y chromosome lampbrush loop in Drosophila spermatocytes. Chromosoma. 1996; 105(5):285–92. PMID: 8939821

55. Sanders C, Smith DP. LUMP is a putative double-stranded RNA binding protein required for male fertility in Drosophila melanogaster. PLoS One. 2011; 6(8):e24151. https://doi.org/10.1371/journal.pone.0024151 PMID: 21912621

56. Gerbasi VR, Preall JB, Golden DE, Powell DW, Cummins TD, Sontheimer EJ. Blanks, a nuclear siRNA/dsRNA-binding complex component, is required for Drosophila spermiogenesis. Proceedings of the National Academy of Sciences. 2011; 108(8):3204–9. https://doi.org/10.1073/pnas.1009781108 PMID: 21300896

57. Bonaccorsi S, Gatti M, Pisano C, Lohe A. Transcription of a satellite DNA on two Y chromosome loops of Drosophila melanogaster. Chromosoma. 1990; 99(4):260–6. PMID: 2119983.

58. Piergentili R. Multiple roles of the Y chromosome in the biology of Drosophila melanogaster. ScientificWorldJournal. 2010; 10:1749–67. https://doi.org/10.1100/tsw.2010.168 PMID: 20842320.

59. Davis MB, Sun W, Standiford DM. Lineage-specific expression of polypyrimidine tract binding protein (PTB) in Drosophila embryos. Mech Dev. 2002; 111(1–2):143–7. PMID: 11804786.

60. Robida M, Sridharan V, Morgan S, Rao T, Singh R. Drosophila polypyrimidine tract-binding protein is necessary for spermatid individualization. Proc Natl Acad Sci U S A. 2010; 107(28):12570–5. Epub 2010/07/10. https://doi.org/10.1073/pnas.1007935107 PMID: 20616016

61. Robida MD, Singh R. Drosophila polypyrimidine-tract binding protein (PTB) functions specifically in the male germline. EMBO J. 2003; 22(12):2924–33. https://doi.org/10.1093/emboj/cdg301 PMID: 12805208

62. Castrillon DH, Gonczy P, Alexander S, Rawson R, Eberhart CG, Viswanathan S, et al. Toward a molecular genetic analysis of spermatogenesis in Drosophila melanogaster: characterization of male-sterile mutants generated by single P element mutagenesis. Genetics. 1993; 135(2):489–505. PMID: 8244010

63. Fabian L, Brill JA. Drosophila spermiogenesis: Big things come from little packages. Spermatogenesis. 2012; 2(3):197–212. https://doi.org/10.4161/spmg.21798 PMID: 23087837

64. Fatima R. Drosophila Dynein intermediate chain gene, Dic61B, is required for spermatogenesis. PLoS One. 2011; 6(12):e27822. https://doi.org/10.1371/journal.pone.0027822 PMID: 22145020

65. Gepner J, Hays TS. A fertility region on the Y chromosome of Drosophila melanogaster encodes a dynein microtubule motor. Proc Natl Acad Sci U S A. 1993; 90(23):11132–6. PMID: 8248219

66. Timakov B, Zhang P. Genetic analysis of a Y-chromosome region that induces triplosterile phenotypes and is essential for spermatid individualization in Drosophila melanogaster. Genetics. 2000; 155(1):179–89. PMID: 10790393

67. Liao SE, Ai Y, Fukunaga R. An RNA-binding protein Blanks plays important roles in defining small RNA and mRNA profiles in Drosophila testes. Heliyon. 2018; 4(7):e00706. https://doi.org/10.1016/j.heliyon.2018.e00706 PMID: 30094376

68. Hoskins RA, Carlson JW, Wan KH, Park S, Mendez I, Galle SE, et al. The Release 6 reference sequence of the Drosophila melanogaster genome. Genome Res. 2015; 25(3):445–58. https://doi.org/10.1101/gr.185579.114 PMID: 25589440

69. Lin TY, Viswanathan S, Wood C, Wilson PG, Wolf N, Fuller MT. Coordinate developmental control of the meiotic cell cycle and spermatid differentiation in Drosophila males. Development. 1996; 122(4):1331–41. PMID: 8620860.

70. White-Cooper H, Schafer MA, Alphey LS, Fuller MT. Transcriptional and post-transcriptional control mechanisms coordinate the onset of spermatid differentiation with meiosis I in Drosophila. Development. 1998; 125(1):125–34. PMID: 9389670.

71. Beall EL, Lewis PW, Bell M, Rocha M, Jones DL, Botchan MR. Discovery of tMAC: a Drosophila testis-specific meiotic arrest complex paralogous to Myb-Muv B. Genes Dev. 2007; 21(8):904–19. https://doi.org/10.1101/gad.1516607 PMID: 17403774

72. Lu C, Fuller MT. Recruitment of Mediator Complex by Cell Type and Stage-Specific Factors Required for Tissue-Specific TAF Dependent Gene Activation in an Adult Stem Cell Lineage. PLoS Genet. 2015; 11(12):e1005701. https://doi.org/10.1371/journal.pgen.1005701 PMID: 26624996

73. Ayyar S. Drosophila TGIF is essential for developmentally regulated transcription in spermatogenesis. Development. 2003; 130(13):2841–52. https://doi.org/10.1242/dev.00513 PMID: 12756169

74. Doggett K, Jiang J, Aleti G, White-Cooper H. Wake-up-call, a lin-52 paralogue, and Always early, a lin-9 homologue physically interact, but have opposing functions in regulating testis-specific gene expression. Dev Biol. 2011; 355(2):381–93. https://doi.org/10.1016/j.ydbio.2011.04.030 PMID: 21570388

75. Jiang J. Transcriptional activation in Drosophila spermatogenesis involves the mutually dependent function of aly and a novel meiotic arrest gene cookie monster. Development. 2003; 130(3):563–73. https://doi.org/10.1242/dev.00246 PMID: 12490562

76. Jiang J, Benson E, Bausek N, Doggett K, White-Cooper H. Tombola, a tesmin/TSO1-family protein, regulates transcriptional activation in the Drosophila male germline and physically interacts with always early. Development. 2007; 134(8):1549–59. https://doi.org/10.1242/dev.000521 PMID: 17360778

77. Perezgasga L, Jiang J, Bolival B Jr., Hiller M, Benson E, Fuller MT, et al. Regulation of transcription of meiotic cell cycle and terminal differentiation genes by the testis-specific Zn-finger protein matotopetli. Development. 2004; 131(8):1691–702. https://doi.org/10.1242/dev.01032 PMID: 15084455.

78. Hiller M, Chen X, Pringle MJ, Suchorolski M, Sancak Y, Viswanathan S, et al. Testis-specific TAF homologs collaborate to control a tissue-specific transcription program. Development. 2004; 131(21):5297–308. https://doi.org/10.1242/dev.01314 PMID: 15456720.

79. Laktionov PP, White-Cooper H, Maksimov DA, Belyakin SN. Transcription factor Comr acts as a direct activator in the genetic program controlling spermatogenesis in D. melanogaster. Molecular Biology. 2014; 48(1):130–40. https://doi.org/10.1134/s0026893314010087

80. Chen X, Hiller M, Sancak Y, Fuller MT. Tissue-specific TAFs counteract Polycomb to turn on terminal differentiation. Science. 2005; 310(5749):869–72. https://doi.org/10.1126/science.1118101 PMID: 16272126.

81. Hiller MA, Lin TY, Wood C, Fuller MT. Developmental regulation of transcription by a tissue-specific TAF homolog. Genes Dev. 2001; 15(8):1021–30. https://doi.org/10.1101/gad.869101 PMID: 11316795

82. Hess O, Meyer GF. Chromosomal differentiations of the lampbrush type formed by the Y chromosome in Drosophila hydei and Drosophila neohydei. J Cell Biol. 1963; 16:527–39. PMID: 13954225

83. Meyer GF, Hess O, Beermann W. [Phase specific function structure in spermatocyte nuclei of Drosophila melanogaster and their dependence of Y chromosomes]. Chromosoma. 1961; 12:676–716. PMID: 14473096.

84. Zhang J, Landick R. A Two-Way Street: Regulatory Interplay between RNA Polymerase and Nascent RNA Structure. Trends Biochem Sci. 2016; 41(4):293–310. https://doi.org/10.1016/j.tibs.2015.12.009 PMID: 26822487

85. Fitz J, Neumann T, Pavri R. Regulation of RNA polymerase II processivity by Spt5 is restricted to a narrow window during elongation. EMBO J. 2018; 37(8). https://doi.org/10.15252/embj.201797965 PMID: 29514850

86. Liu CR, Chang CR, Chern Y, Wang TH, Hsieh WC, Shen WC, et al. Spt4 is selectively required for transcription of extended trinucleotide repeats. Cell. 2012; 148(4):690–701. https://doi.org/10.1016/j.cell.2011.12.032 PMID: 22341442.

87. Voynov V, Verstrepen KJ, Jansen A, Runner VM, Buratowski S, Fink GR. Genes with internal repeats require the THO complex for transcription. Proc Natl Acad Sci U S A. 2006; 103(39):14423–8. https://doi.org/10.1073/pnas.0606546103 PMID: 16983072

88. Wagner EJ, Garcia-Blanco MA. Polypyrimidine tract binding protein antagonizes exon definition. Mol Cell Biol. 2001; 21(10):3281–8. https://doi.org/10.1128/MCB.21.10.3281-3288.2001 PMID: 11313454

89. Valcarcel J, Gebauer F. Post-transcriptional regulation: the dawn of PTB. Curr Biol. 1997; 7(11):R705–8. PMID: 9382788.

90. Sawicka K, Bushell M, Spriggs KA, Willis AE. Polypyrimidine-tract-binding protein: a multifunctional RNA-binding protein. Biochem Soc Trans. 2008; 36(Pt 4):641–7. https://doi.org/10.1042/BST0360641 PMID: 18631133.

91. Kafasla P, Mickleburgh I, Llorian M, Coelho M, Gooding C, Cherny D, et al. Defining the roles and interactions of PTB. Biochem Soc Trans. 2012; 40(4):815–20. https://doi.org/10.1042/BST20120044 PMID: 22817740.

92. Shepard S, McCreary M, Fedorov A. The peculiarities of large intron splicing in animals. PLoS One. 2009; 4(11):e7853. https://doi.org/10.1371/journal.pone.0007853 PMID: 19924226

93. Rothe M, Pehl M, Taubert H, Jackle H. Loss of gene function through rapid mitotic cycles in the Drosophila embryo. Nature. 1992; 359(6391):156–9. https://doi.org/10.1038/359156a0 PMID: 1522901.

94. Shermoen AW, O'Farrell PH. Progression of the cell cycle through mitosis leads to abortion of nascent transcripts. Cell. 1991; 67(2):303–10. PMID: 1680567

95. Chen D, McKearin DM. A discrete transcriptional silencer in the bam gene determines asymmetric division of the Drosophila germline stem cell. Development. 2003; 130(6):1159–70. PMID: 12571107.